# Low-Complexity Blind Interference Suppression With Reconfigurable Antennas

Milad Johnny<sup>®</sup> and Alireza Vahid<sup>®</sup>, Senior Member, IEEE

Abstract—We present a new low-complexity interference management algorithm that exploits reconfigurable antennas, removes most of the interference signal power in a K-user interference channel, and achieves the promised but unrealized gain of interference alignment in low-to-medium signal-tonoise ratio (SNR) range. The reconfigurable antenna includes several elements, each controlled individually using a radio frequency (RF) switch. The antenna has only one RF chain, resulting in simple hardware design and enabling low-complexity algorithms. We exploit space-time diversity to find two separate combinations of activating or deactivating antenna elements to allow for interference neutralization/elimination. Finding such states is a cumbersome task for which we develop novel, efficient algorithms. We further devise simple encoding and decoding with short precoder length to exploit the benefits of our designs. Our implementation does not rely on channel state information at the transmitters; works at finite signal-to-noise ratios, unlike the typical degrees-of-freedom results; and works in slow-fading environments. We calculate the average achievable rates, the minimum number of elements to reach a specific level of interference suppression, and we provide outage analysis of our technique.

Index Terms—Interference suppression, binary switched antennas, single RF chain, outage capacity, no CSIT.

# I. INTRODUCTION

THE current trends in wireless networking point to a dramatic increase in the data-rate demands and the number wireless devices. To meet such fast-pace changes for mobile traffic and number of devices, network operators need to scale up networks to provide the required throughput while containing costs and other overheads. The current solution for the next generation of wireless systems is network densificiation with which interference would become the bottleneck for network capacity improvements and scalability.

To manage interference and to scale up the number of users, the current approach is to avoid interference both in cellular

Manuscript received February 7, 2021; revised June 14, 2021 and September 1, 2021; accepted September 16, 2021. Date of publication October 4, 2021; date of current version April 11, 2022. The work of Alireza Vahid was supported in part by NSF under Grant ECCS-2030285 and Grant CNS-2106692. The associate editor coordinating the review of this article and approving it for publication was M. Kountouris. (Corresponding author: Alireza Vahid.)

Milad Johnny is with the Department of Electrical Engineering, Kermanshah University of Technology (KUT), Kermanshah 6715685420, Iran (e-mail: milad.johnny@gmail.com).

Alireza Vahid is with the Department of Electrical Engineering, University of Colorado at Denver, Denver, CO 80204 USA (e-mail: alireza.vahid@ucdenver.edu).

Color versions of one or more figures in this article are available at https://doi.org/10.1109/TWC.2021.3115696.

Digital Object Identifier 10.1109/TWC.2021.3115696

and WiFi connectivity. For example, in 5G, the idea is to create narrowband frequency slots, which mimic single carrier communication, and leverage spatial dimension extensively to load concurrently many users on the same narrowband frequency slot [1]. However, even with spatial division multiplexing (SDMA), there are multiple problem: (1) even with massive multiple-input multiple-output (MIMO), antenna side-lobes still cause interference, (2) users collocated in the same spatial direction cannot be serviced simultaneously, (3) we lose the gains due to multipath diversity [2], and (4) the number of users is limited by the number of spatial dimensions.

Beyond attempts to avoid interference in wireless systems, such as SDMA, there are theoretical results that aim to exploit and eliminate interference with schemes such as interference alignment (IA) [3], [4]. The main idea behind IA is to confine the interfering signals at each receiver to a subspace (linearly) independent of the desired signal. The typical metric for evaluating the performance of IA techniques is degrees-offreedom (DoF), which is the prelog factor in achievable rates. Thus, by definition DoF is not a suitable metric for real-world low-to-medium signal-to-noise ratio (SNR) values. Nonetheless, in terms of DoF, IA promises scaling gains over orthogonalization techniques. Unfortunately, however, many existing IA schemes require significant coordination, for example in the form of accurate and global channel state information (CSI) at the nodes whether instantaneous or delayed, and complicated encoding and decoding, further restricting their practicality [5], [6].

In this work, we present a low-complexity approach to recover or even exceed the significant promised gains of interference alignment in low-to-medium SNR values. The low-complexity is reflected both in hardware structure and in algorithms. More precisely, we focus on a simple array antenna with only one RF chain, which implies our schemes cannot rely on the benefits of joint-processing. Further, we assume no CSI is available to the transmitters and each receiver is only aware of its local channels. In fact, the only coordination we require is the synchronization among the transmitters, which is already given in current long-term evolution (LTE) and WiFi protocols [7]. Interestingly, we observe that the proposed methodology achieves the asymptotic high-SNR outer-bounds of interference alignment in *low-to-medium* SNR and without

1536-1276 © 2021 IEEE. Personal use is permitted, but republication/redistribution requires IEEE permission. See https://www.ieee.org/publications/rights/index.html for more information.

<sup>&</sup>lt;sup>1</sup>In this context, joint-processing refers to mixing the outcomes of multiple RF chains with desired coefficients.

accessing channel state information at transmitters (CSIT), but the performance saturates in higher SNR values.

Our contributions can be summarized as follows: (i) we present a low-complexity, low-coordination distributed interference management technique that achieves the promised gains of IA in low-to-medium SNR values. Our solution includes new encoding and decoding strategies and algorithmic solutions to configure the array antenna; (ii) we analyze the complexity of the algorithms to reconfigure the antenna as it is the main bottleneck for scalability of the ideas, and we present novel implementation motivated by genetic solutions; (iii) we evaluate the outage capacity of the solutions and evaluate the results through simulations; and (iv) we derive bounds on the interplay between the number of users that needs to be supported vs. the required number of elements in the array antenna.

Related work: Blind Interference Alignment (BIA) of [8] shows that if the channel coherence has some specific structure, then the benefits of IA can be still attained without accessing CSI at the transmitters. To control channel coherence times, one idea is to use multi-mode switching antennas (also known as reconfigurable antennas) at the receivers [9], [10]. In this case, the receivers are equipped with an antenna that can switch among r different reception modes and the transmitters use specifically designed precoders to create the transmission signals. Using this approach, a sum DoF of 6/5 is achievable in 3-user ICs. This approach is also generalized to K-user interference channels to show that when the number of users goes to infinity, the sum DoF goes to the value of  $\sqrt{K}/2$  [11]. In [12], the authors use reconfigurable antennas structure to implement blind interference alignment for a 2-user multiple-input single-output (MISO) broadcast channel. In [13], the authors propose a method to implement IA in a multipath fading environment based on a new receive antenna structure, but there is no detailed analysis as to how receivers may obtain the necessary CSI. The scheme of [14] relies on the availability of time-varying, independent channel coefficients drawn from a discrete uniform distribution. In [15], the authors propose a scheme in which receivers create nulls in different spatial directions, while maintaining the desired signal's power above some threshold. This scheme relies on the presence of line-of-sight channels and thus, is not suitable for dense environments. Finally, to complement the efforts on receiver designs, in [16], [17] we demonstrated how to embed information in coherence time fluctuations induced by transmit antennas, which requires complex calculations to optimize the average achievable rates. Finally, we note that such ideas are not limited to Gaussian channels and also appear in discrete channels [18]-[22] and in multi-layer networks [23], [24].

# II. RECONFIGURABLE ANTENNA STRUCTURE AND SYSTEM MODEL

We focus on a multi-cell communication system modeled as a K-user interference channel with no cooperation among the transmitters. In this section, we present the channel model and the reconfigurable antenna structure.

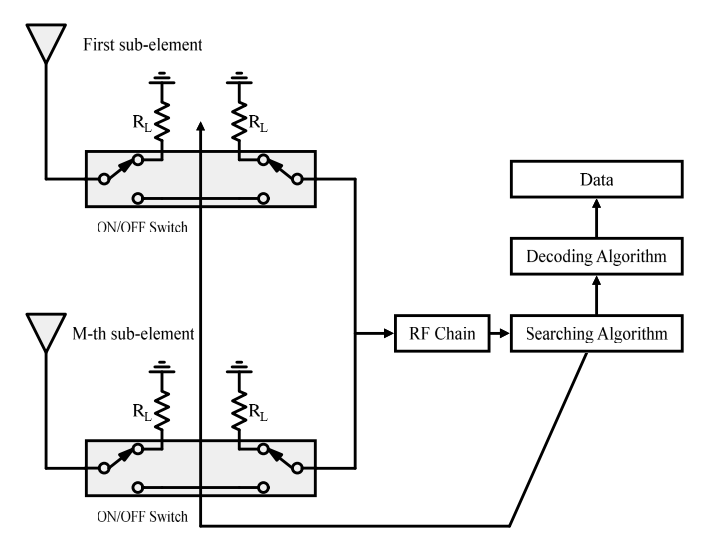


Fig. 1. The receiver structure can control the reception mode of its antenna by its RF switches.

## A. Antenna Structure

Fig. 1 shows the receiver structure including an antenna with M elements and one RF chain. Such an antenna structure is referred to as reconfigurable antennas [25]-[28]. The goal is to find antenna configurations across which the interfering signals can be aligned in a subspace linearly independent of the desired signal. Implementing this reception structure can increase the transmission rates without channel state information at the transmitters. The receiver can control the RF switches to scan through and create  $2^M$  different states. Basically, the role of these RF switches is to connect the power combiner network to each of the elements or to a matched load. When RF switch i is in the active state  $(s_i = 1)$ , the power combiner network is connected to its corresponding element and it can receive RF signals from the environment. When RF switch i is in the inactive mode ( $s_i = 0$ ), the element is connected to a passive matched load  $(R_L)$ , and the power combiner is disconnected from the environment. All elements are connected through a power combiner, the signals are filtered, amplified, and down-converted using a single RF chain as in Fig. 1. Thus, there is no need to implement structures with several RF chains. This antenna may be modified depending on practical constraints, and the desired characteristics are:

- The elements are spaced no less than  $\lambda/2$  (where  $\lambda$  is the wavelength) to receive the RF signals without affecting each other (i.e. coupling) and increase spatial diversity;
- The receiver controls the elements using individual RF switches;
- When inactive, both the element and the RF feed are connected to matched loads. The former cancels scattering from adjacent elements and the latter cancels reflection from the RF network.

# B. System Model

We consider a K-user interference channel (IC) with K transmitters  $\mathrm{TX}_j$ , and K receivers  $\mathrm{RX}_i$ ,  $i,j \in \mathcal{K} = \{1,\ldots,K\}$ . As the main focus of this work is on enabling

interference suppression at the receivers, we assume the transmitters have omni-directional antennas, and are only aware of the channel statistics but not the actual channel realizations. This model is commonly referred to as no channel state information at the transmitters or no CSIT for short. Each receiver is equipped with the antenna structure described in the previous subsection. Each element of the receiver antenna receives a signal from all of the transmitters. In Fig. 1, each receiver antenna consisted of M sub-elements, which are connected using RF switches and a power combiner. We can model the reception state of each receiver antenna by M-tuple of  $S^{[i]} = (s_1^{[i]}, \dots, s_M^{[i]}), s_m \in \{0, 1\}$ . When the value of  $s_m^{[i]}=1$ , the *m*-th element of receiver antenna at *i*-th receiver is connected to the RF network while  $s_m^{[i]} = 0$  means that the m-th element of receiver antenna at i-th receiver is disconnected from the RF network and connected to a matched load to minimize the effect of scattering from unmatched load element. We assume each receiver learns the incoming channel gains through a training phase and beyond that is only aware of the channel statistics. This model is commonly referred to as local channel state information at the receivers or no CSIR for short.

As a final point, we note that for an antenna with M subelements wherein each subelement can be turned on or off individually, we will have a total of  $2^M$  possible configurations at each time. However, it is not necessary to perform measurements for all such combinations, which would make the training phase unnecessarily long. In fact, during a training phase, the transmitters could be scheduled in non-overlapping (at least with high probability) time slots and then, each receiver estimates the M channel values associated with its subelements from the active transmitter. We can then compute the aggregate channel values of any configuration offline.

# III. TRANSMISSION STRATEGY

## A. Encoding Strategy

We consider the problem of data transmission in an unknown time variant channel. We assume that each transmitter uses a digital modulation scheme in which Q different symbols can be transmitted. We assume symbols (or messages) are uniformly distributed and with time duration of  $T_s$  (the symbol duration). Transmitter  $\mathrm{TX}_j$  wishes to send uniformly distributed message  $W^{[j]} \in \mathcal{W}^{[j]}$  to  $\mathrm{RX}_j, j \in \mathcal{K}$ , over n uses of the channel with time duration of  $nT_s$ . The transmission rate for the above digital modulation technique can be calculated from the following relation:

$$R^{[j]} = \frac{\log_2 Q}{T_c}, \ |\mathcal{W}^{[j]}| = 2^{nR^{[j]}}.$$
 (1)

We assume that the messages at the transmitters are independent from each other and the channel gains. Each transmitter is subject to the total average transmission power constraint of  $P_t = \frac{\mathcal{E}}{T_s}$ . Transmitter  $\mathrm{TX}_j$  encodes its message  $W^{[j]}$  using the encoding function  $X^{[j]}(t) = e_j\left(W^{[j]}\right)$  where  $j \in \mathcal{K}$  and  $e_j\left(W^{[j]}\right)$  is an one to one function from messages to the stream of symbols at  $\mathrm{TX}_j$ . In simpler notation, we have the

following relation:

$$X^{[j]}(t) = e_j\left(W^{[j]}\right) = \sum_i U_{q_j}^{[j]}(t - iT_s), \ 1 \le q_i \le Q, \quad (2)$$

where  $U_{q_i}^{[j]}\left(t-iT_s\right)$  represents transmission symbol in  $i^{\rm th}$  transmission time.

Definition 1: We define the transmission block of  $B_b, b \in \{1,\dots,n\}$  in which all transmitters repeat their transmission symbols 2 times. Therefore the total transmission time of each block is  $2T_s$  and if i has even value at  $j^{th}$  transmitter, we can assume that  $U_{qi}^{[j]} = U_{qi+1}^{[j]}$ . Therefore, in this case the transmission rate of equation 1 at  $\mathrm{TX}_j$  can be calculated as  $R^{[i]} = \frac{\log Q}{2T_s}$ .

## B. Received Signal Model

The output of each of the encoder functions from different transmitters is sent through a channel that has unknown impulse response at different sub-elements of the receiver antennas, and the noise power is added to the received signal. Thus, the received signal depends on the state of the switches at  $RX_i$ , and for  $1 \le m \le M$ ,  $s_m^{[i]} \in \{0,1\}$ , is given by:

$$Y^{[i]}(t) = \sum_{j \in \mathcal{K}} \sum_{m=1}^{M} s_m^{[i]} h_{mj}^{[i]}(t) X^{[j]}(t) + Z^{[i]}(t),$$
 (3)

where  $s_m^{[i]}$  represents the state of the  $m^{\rm th}$  RF switch,  $\mathcal{K}$  indicates the subset of active transmitters at the  $B^{th}$  transmission block,  $h_{mj}^{[i]}(t)$  shows channel coefficient between  $\mathrm{TX}_j$  and the  $m^{\rm th}$  subelement of the receiver antenna at  $\mathrm{RX}^{[i]}$ , and  $Z^{[i]}(t)$  indicates additive white Gaussian noise with zero mean and unit variance. For simplicity of notation, we can define the channel coefficient vector as follows:

$$\bar{\mathbf{H}}^{[ij]} = \left[ h_{1\ j}^{[i]}, h_{2\ j}^{[i]}, \dots, h_{Mj}^{[i]} \right], \ j \in \mathcal{K}.$$
 (4)

where all the channel coefficients at the baseband have real values with specific distribution.

Remark 1: In practice, channel values are complex. Our results extend to this case as the real and the imaginary parts can be analyzed independently. Therefore, for simplicity, we assume real-valued channel gains. For our antenna, we could use independent RF networks and switches, as well as an oscillator with a 90-degree phase-shifted version for down-converting.

# C. Decoding Strategy

We assume that each receiver  $RX_i$  is aware of its channel state information and decodes its intended message  $W^{[i]} \in \mathcal{W}^{[i]}$  using the decoding function  $\hat{W}^{[i]} = \phi_i \left( \bar{\mathbf{Y}}^{[i]}, \operatorname{SI}_{Rx_i} \right)$ , where  $\operatorname{SI}_{Rx_i}$  is the side information available to the receiver (in this case CSI). Then, the decoding error probability at receiver  $RX_i$  is given by

$$\lambda_e^{[i]}(n) = \mathbb{E}\left[\Pr\left(\hat{W}^{[i]} \neq W^{[i]}\right)\right],$$
 (5)

where the expectation is over the random choice of messages. The  $i^{\rm th}$  receiver has access to channel gains  $h_{mj}^{[i]}, 1 \leq m \leq M, j \in \mathcal{K}$ . Therefore, each receiver has only access to

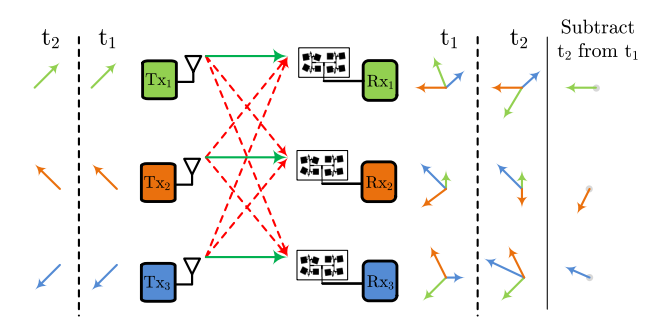


Fig. 2. A 3-user IC in which receivers are equipped with the proposed structure each with M=8 sub-elements. As it indicated in this figure each transmitter repeats its symbol two times and the receivers antennas try to find two reception channel states where all the cross channels (interference channel) remain constant while the direct channels change.

the channel gains connected to it. At the end of training signal transmission phase, receiver  $\mathrm{RX}_i,\ i\in\mathcal{K}$ , uses a search algorithm to find two different reception states,  $S^{[i]}(k_1)$  and  $S^{[i]}(k_2)$ , such that the following conditions at  $\mathrm{RX}_i$  are satisfied:

$$\sum_{i \in \mathcal{K}, i \neq i} |\sum_{m=1}^{M} s_m^{[i]}(k_1) h_{mj}^{[i]} - \sum_{m=1}^{M} s_m^{[i]}(k_2) h_{mj}^{[i]}|^2 \le \delta^2, \quad (6)$$

$$\left|\sum_{m=1}^{M} s_{m}^{[i]}(k_{1}) h_{mi}^{[i]} - \sum_{m=1}^{M} s_{m}^{[i]}(k_{2}) h_{mi}^{[i]}\right|^{2} \ge \Delta_{i}^{2},\tag{7}$$

where  $s_m^{[i]}(k) \in \{0,1\}$  indicates the switching state at the  $m^{th}$  sub-element of the  $i^{th}$  receiver. The inequality in (6) indicates that all the cross links in the two separate states of  $S^{[i]}(k_1)$  and  $S^{[i]}(k_2)$  have the same value to within a small value of  $\delta$ . Relation (7) indicates that the difference of all the direct links in two separate state of  $S^{[i]}(k_1)$  and  $S^{[i]}(k_2)$  is greater than  $\Delta_i$ . When  $\left(\frac{\Delta_i}{\delta}\right)^2$  has a larger value, the portion of desired signal power to the interference signal power at  $RX_i$  has greater value. Both relations (6) and (7) can be expressed without subtraction equations as follows:

$$\sum_{j \in \mathcal{K}, j \neq i} |\sum_{m=1}^{M} \gamma_m^{[i]}(k_1) h_{mj}^{[i]}|^2 \le \delta^2,$$
 (8)

$$|\sum_{i=1}^{M} \gamma_{m}^{[i]} h_{mi}^{[i]}|^{2} \ge \Delta_{i}^{2}, \tag{9}$$

where  $\gamma^{[i]} \in \{-1,0,1\}$ . Therefore, we have  $3^M$  different reception states to control the receiver antenna. Intuitively, if all the direct links change (the transmission link between  $\mathrm{TX}_j$  and  $\mathrm{RX}_j$ ) and all the cross links (the transmission link between  $\mathrm{TX}_j$  and  $\mathrm{RX}_i$  where  $i \neq j$ ) remain the same with the small value of  $\delta$ , the receivers can decode their desired symbols by a simple subtraction of two sequential received signal at each block (see Fig. 2). We accomplish this goal by finding proper reception states using the proposed antenna structure.

TABLE I
RANDOM POSITIONS OF DIFFERENT TRANSMITTERS AND RECEIVERS

user index	mean TX position	mean RX position	Variance
1	$(-100\lambda, 150 \lambda)$	$(100\lambda, 150 \lambda)$	$\sigma_x^2, \sigma_y^2 = 10\lambda$
2	$(-100\lambda, 50 \lambda)$	$(100\lambda, 50 \lambda)$	$\sigma_x^2, \sigma_y^2 = 10\lambda$
3	$(-100\lambda, -50 \lambda)$	$(100\lambda, -50 \lambda)$	$\sigma_x^2, \sigma_y^2 = 10\lambda$
4	$(-100\lambda, -150 \lambda)$	$(100\lambda, -150 \lambda)$	$\sigma_x^2, \sigma_y^2 = 10\lambda$

# D. 4-User Example

As a motivating example, consider a 4-user fully-connected interference channel in which transmitters and receivers are placed randomly. We assume each receiver is equipped with the antenna of Fig. 1 with M=12 sub-elements. We further assume that all the sub-elements with  $0~{\rm dB}$  gain, and the following positions:

$$\left(x_r^{[i]} + \frac{\lambda}{2}p, y_r^{[i]} + \frac{\lambda}{2}q, z_r^{[i]}\right). \tag{10}$$

where  $0 \le p \le 3$ ,  $0 \le q \le 2$ ,  $1 \le i \le 4$ , and  $\left(x_r^{[i]}, y_r^{[i]}, z_r^{[i]}\right)$  indicates the position of the  $i^{\text{th}}$  receiver  $(1 \le i \le 4)$ . In this case, we assume all the antenna sub-elements are located on a  $3 \times 4$  square mesh. The positions of all the transmitters and receivers are Gaussian random variables with some means and variances which are indicated in table I. For simplicity, we assume each transmitter has a simple antenna at  $\left(x_t^{[j]}, y_t^{[j]}, z_t^{[j]}\right)$ . Also, we assume all the transmitters have 0 dB gain antennas. We assume free space attenuation and phase shifting equations can model the channel gains among transceivers antennas as follows:

$$h_{mj}^{[i]} = \sqrt{G^{[j]} G_m^{[i]}} \left( \frac{\lambda}{4\pi d_{mj}^{[i]}} \right) e^{-\frac{2\pi}{\lambda} d_{mj}^{[i]} \sqrt{-1}}$$
 (11)

where  $d_{mj}^{[i]}$  and  $h_{mj}^{[i]}$  indicate the distance and the channel value between  $\mathrm{TX}_j$  and  $m^{th}$  element of  $i^{th}$  receiver, respectively. Also,  $G^{[j]}$  and  $G_m^{[i]}$  indicate  $j^{th}$  transmitter and  $m^{th}$  element of i<sup>th</sup> receiver sub-element antenna gains. Setting proper switching patterns at receivers, we can maximize the achievable signal-to-interference-plus-noise ratio (SINR). In this example, we simulated the results for 100 randomly generated positions for each of the transmitters and the receivers, and we calculated the average transmission rate for different methods. Fig. 3 shows the average achievable rates for different schemes with the random distribution positions and the parameters given in Table I, when the transmitters have equal power. In this figure, the red dashed line is the performance of treating-interference-as-noise (TIN). For low SNR values (i.e., SNR below 2.7 dB), we achieve better performance with TIN in comparison to other schemes, because in compared with noise power, interference signals have negligible effect on the desired received signal. Since all the transmitters have the same power, TIN is not the best solution at higher SNR values where the interference signals have more power. The inverted-triangle solid purple curve is the achievable rate of an orthogonalization strategy, such as TDMA, and is equivalent

 $<sup>^2 \</sup>text{Choosing}$  smaller values for  $\delta$  and higher values for  $\Delta_i^2$  results in more restrictive conditions at  $\mathrm{RX}_i$  and the chance of meeting the above requirements diminishes.

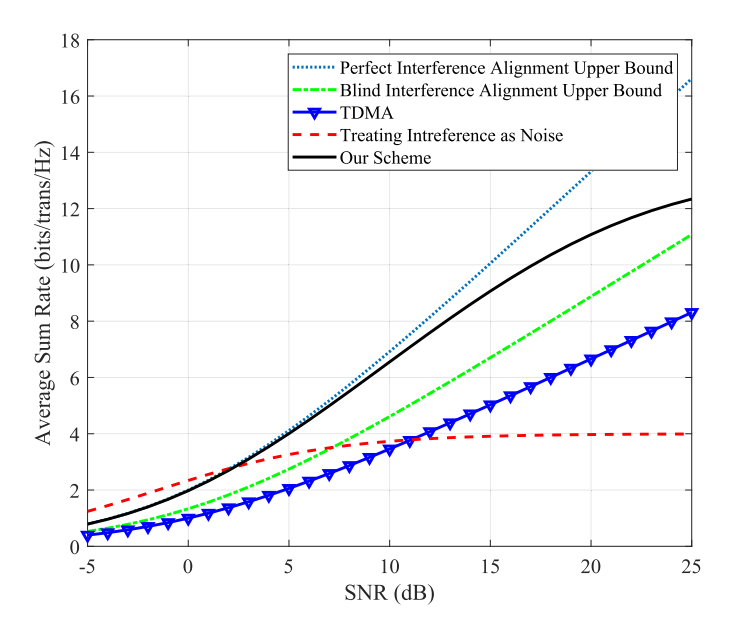


Fig. 3. A comparison between different transmission schemes with channel coefficients which are extracted from the transmitters/receivers with random positions and simple free space calculation.

to the average capacity of a single point-to-point channel. The dotted dashed green curve shows the upper-bound on the achievable sum-rate of the Blind Interference Alignment scheme presented in [11] given by  $d_{\text{sum}} = \frac{Kr}{r^2 - r + K} = \frac{4}{3}, r = 2, K = 4$ . The dotted blue curve indicates the upper-bound on the achievable DoF of 4-user interference channel (i.e., sum DoF of 2). Finally, the solid black curve corresponds to our transmission and reception strategy with the switching states indicated earlier, which are functions of the channel states. Thus, for a wide operational SNR range, our scheme significantly outperforms the other schemes. As we discuss later in Section IV-B, our gains saturate at higher SNR values.

Remark 2: Most existing results on interference alignment are developed for the asymptotic degrees-of-freedom analysis. However, rather unfortunately, there is no simple way of optimizing these results to work for finite SNR values. Even for this case with centralized transmitter [29], the extension to finite SNR values was highly non-trivial [30], [31]. The challenges are multi-fold. First going to finite SNR requires careful allocation of retransmission bits to accommodate power level differences, something that does not appear in degrees-offreedom analysis. Further, for the problem of interest, capacity bounds are needed, which was doable for MISO Gaussian broadcast channels. However, the capacity of the K-user interference channels, even when K = 2, is still open. Finally, when all these are possible, as was the case for the MISO Gaussian broadcast channel, the extension of the existing results only provided a constant-gap approximation.

# E. Further Assumptions

As stated earlier,  $\lambda$  denotes the wavelength of the transmission signal. At each receiver antenna, we assume the sub-elements are spaced at least  $\frac{\lambda}{2}$  apart from each other, so that the channel values are independent. Therefore, we can

assume that all the channel values of  $h_{mj}^{[i]}(t)$  are independent from each other and at each receiver, we have  $K\times M$  independent channel coefficients. In this paper, we assume cellular communication network with frequency reuse factor of  $N=p^2+pq+q^2,\ p,q\in\mathbb{W}^3$  in which each receiver is affected by multiple interferers. In this case, the distance of the closest interfering transmitter to the center of each cell can be calculated from  $D=R\sqrt{3N}$  where R is the radius of each cell [32]. The minimum ratio of the desired signal-to-interference power from one interfering source is given by:

$$SIR = \left(\frac{D}{R}\right)^{\alpha} = (3N)^{\frac{\alpha}{2}}, \tag{12}$$

where  $\alpha$  is path loss exponent, which for the free space environment equals to 2 and for more practical cases, is greater than 2. For instance, in urban areas  $\alpha$  ranges from 3 to 4.

# IV. NUMBER OF SUB-ELEMENTS VS. TRANSMISSION RATES

In this section, we evaluate the minimum number of sub-elements in our antenna structure to guarantee a sufficiently large value for  $\frac{\Delta^2}{\delta^2}$  at the receivers. The minimum number of required receiver elements and the switching modes are functions of  $\delta_{\max}$  and the channel variance  $\sigma_H^2$ . The channel variance,  $\sigma_H^2$ , can be calculated from the following relation:

$$\sigma_H^2 = \int_{-\infty}^{\infty} h^2 f_H(h) dh, \tag{13}$$

where in the above equation h is the channel value and  $f_H(h)$  represents channel distribution. For simplicity of our analysis, we consider the real-valued base-band channel model. Then, all the arguments can be generalized by independently analyzing the in-phase and the quadrature components.

The following lemma (proof in Appendix B) plays an important role in our analysis.

Lemma 1: If  $\bar{\mathbf{H}}^{[ij]}$  is the channel vector between  $\mathrm{TX}_j$  and  $\mathrm{RX}_i$  where all its elements are statistically independent, then, for a given vector  $\bar{\gamma}^{[i]}$  whose elements are drawn randomly and independently from  $\{-1,0,1\}$ , the value of  $\bar{\mathbf{H}}^{[ij]} \cdot \bar{\gamma}^{[i]}$  has the following average variance:

$$v\bar{a}r\left(\bar{\mathbf{H}}^{[ij]}\cdot\bar{\gamma}^{[i]}\right) = \frac{M}{2}\sigma_H^2 \stackrel{\triangle}{=} V \tag{14}$$

where  $\bar{\mathbf{H}}^{[ij]} \cdot \bar{\gamma}^{[i]}$  is the inner product between two vectors of  $\bar{\mathbf{H}}^{[ij]}$  and  $\bar{\gamma}^{[i]}$  of the same size.

The distribution of  $\bar{\mathbf{H}}^{[ij]} \cdot \bar{\gamma}^{[i]}$  has a symmetric bell shape. A simple histogram of this parameter with M=10 is plotted in Figure 4. Based on the following lemma (proof in Appendix C), this distribution can be approximated with a zero-mean Gaussian distribution with similar variance.

Lemma 2: For sufficiently small positive values of  $\delta$ , the probability of finding a vector  $\bar{\gamma}^{[i]}$  to satisfy  $|\bar{\mathbf{H}}^{[ij]} \cdot \bar{\gamma}^{[i]}| < \delta$  can be approximated by

$$\frac{2}{\sqrt{2\pi}}\frac{\delta}{V} - \frac{2}{3\sqrt{2\pi}}\frac{\delta^3}{V^3} + \mathcal{O}\left(\frac{\delta^5}{V^5}\right),\tag{15}$$

<sup>&</sup>lt;sup>3</sup>Whole numbers or non-negative integers.

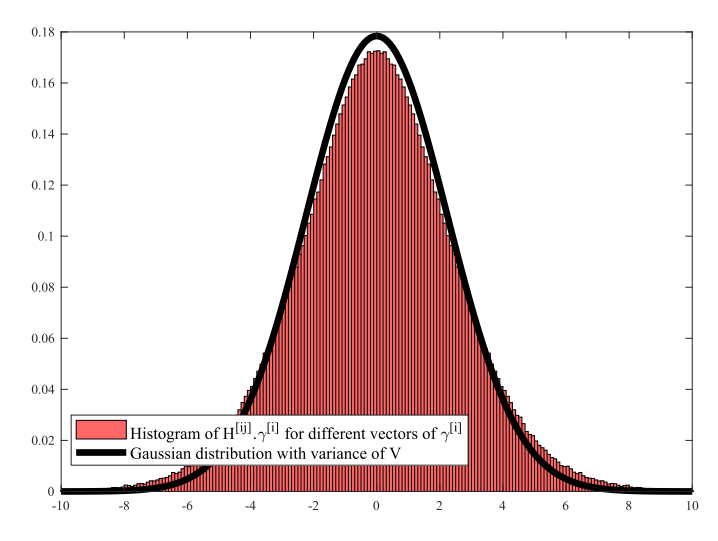


Fig. 4. Comparison between a Gaussian distribution with zero mean and variance  $V = \frac{\sum_{l=0}^{M} \binom{M}{l}(M-l)}{2^{M}} \sigma_{H}^{2}$  and distribution of  $\bar{\mathbf{H}}^{[ij]} \cdot \bar{\gamma}^{[i]}$  for different  $\bar{\gamma}^{[i]}$ 's.

for

$$\sigma \stackrel{\triangle}{=} \sqrt{V},\tag{16}$$

where V is defined in (14), and the Landau notation ("big O") is used in its standard form.

Since  $\delta$  is small, we can ignore the effect higher order terms of  $\frac{\delta}{\sigma}$ . Therefore, we can assume that:

$$p\left(|\bar{\mathbf{H}}^{[ij]}\cdot\bar{\gamma}^{[i]}|<\delta\right) \approx \frac{2}{\sqrt{2\pi}}\frac{\delta}{\sigma} \stackrel{\text{(16)}}{=} \frac{2}{\sqrt{\pi M}}\frac{\delta}{\sigma_H}.$$
 (17)

Therefore, in this case the probability of finding two different switching states of  $S^{[i]}(k_1)$  and  $S^{[i]}(k_2)$  at  $\mathrm{RX}_i$  in which the values of  $\sum_{m=1}^M s_m^{[i]}(k_1) h_{mj}^{[i]}$  and  $\sum_{m=1}^M s_m^{[i]}(k_2) h_{mj}^{[i]}$  are within the value of  $\delta_{\mathrm{max}}$  can be approximated as follows:

$$p\left(|\bar{\mathbf{H}}^{[ij]} \cdot \bar{\gamma}^{[i]}| < \delta_{\max}\right) \approx \frac{2}{\sqrt{\pi M}} \frac{\delta_{\max}}{\sigma_H}, \ i \text{ is a constant}$$
(18)

The probability of satisfying the above condition for all the cross links at  $RX_i$  in the active set of  $\mathcal{K}$  can be approximated as follows where  $j \in \mathcal{K}$  and  $j \neq i$ :

$$p\left(|\bar{\mathbf{H}}^{[ij]}\cdot\bar{\gamma}^{[i]}|<\delta_{\max}\right)\approx\left(\frac{2}{\sqrt{\pi M}}\frac{\delta_{\max}}{\sigma_H}\right)^{|\mathcal{K}|-1}.$$
 (19)

# A. Determining the Minimum Required Number of Sub-Elements

In this subsection, using the previous lemmas, we determine the minimum number of antenna sub-elements to satisfy the interference power to within a maximum threshold  $\delta_{\max}$ . In other words, we find M such that almost surely we have  $|\bar{\mathbf{H}}^{[ij]}\cdot\bar{\gamma}^{[i]}|<\delta_{\max}$ .

Lemma 3: The minimum number of M to almost surely satisfy  $|\bar{\mathbf{H}}^{[ij]} \cdot \bar{\gamma}^{[i]}| < \delta_{\max}$  is

$$\frac{|\mathcal{K}| - 1}{\log 3} \log \left(\frac{\sigma_H}{\delta_{\text{max}}}\right) + c, \tag{20}$$

where c is a function of M and for practical scenarios, is not greater than  $1.5(|\mathcal{K}|-1)$ .

*Proof:* We have  $3^M$  different reception states. In order to align the interference signal power at  $RX_i$ , *i.e.* satisfy (8) and (9) with high probability, we need:

$$3^{M} \left( \frac{2}{\sqrt{\pi M}} \frac{\delta_{\text{max}}}{\sigma_{H}} \right)^{|\mathcal{K}|-1} > 1, \tag{21}$$

resulting in

$$M > \frac{|\mathcal{K}| - 1}{\log 3} \log \left( \frac{\sqrt{\pi M \sigma_H}}{2\delta_{\text{max}}} \right).$$
 (22)

In particular, if  $M \leq 32$  (due to practical limitations), we can relax the right hand-side of the above inequality as  $M > \frac{|\mathcal{K}|-1}{\log 3}\log\left(\frac{\sigma_H}{\delta_{\max}}\right) + 1.5\left(|\mathcal{K}|-1\right)$ . We can conclude that all each receiver should have a minimum number of  $\left\lceil \frac{|\mathcal{K}|-1}{\log 3}\log\left(\frac{\sigma_H}{\delta_{\max}}\right) + 1.5\left(|\mathcal{K}|-1\right) \right\rceil$  elements to align interference signals within the value of  $\delta_{\max}^2$ .

We can rearrange (22) to obtain a bound on  $\delta_{\rm max}$  based on the number of sub-elements:

$$\delta_{\text{max}} < 2^{-\left(\frac{M}{|\mathcal{K}|-1} - 1.5\right)\log 3} \sigma_H. \tag{23}$$

Example: Suppose we have  $|\mathcal{K}|=4$  active transmitters and assume that  $\delta_{\max}=0.1$  and  $\sigma_H^2=1$ . In this case, the minimum number of sub-elements in the receiver antenna, M, would be 11. We note that in a cellular network, we typically expect interference from a small number of nearby base-stations and  $|\mathcal{K}|=4$  is a reasonable assumption.

# B. Average Achievable Sum-Rate

We denote the (physical) distance from transmitter  $TX_j$  to  $RX_i$  by  $d_{ij}$ . Then, the average achievable sum-rate can be calculated by treating the total remaining interference power as noise after the decoding strategy as follows:

$$C_{\text{avg}}^{[i]} = \int_{-\infty}^{+\infty} \frac{1}{4} \log \left( 1 + \frac{\delta^2 P_t / d_{ii}^{\alpha}}{P_n + \delta_{\text{max}}^2 \left( \sum_j \frac{1}{d_{ij}^{\alpha}} \right) P_t} \right) \times f_{\Delta}(\delta) d\delta, \tag{24}$$

where  $j \neq i, j \in \mathcal{K}$ ,  $\alpha$  is the path loss exponent coefficient,  $P_n$  is additive noise power, and from the first lemma  $f_{\Delta}(\delta)$  is Gaussian distribution with zero mean and the variance of  $\frac{M}{2}\sigma_H^2$ . The coefficient  $\frac{1}{4}$  comes from the transmission in two time snapshots and the basic coefficient of channel capacity for point-to-point communication. For a cellular communication network, we can substitute  $d_{kk}$  and  $d_{kj}$  with R and  $R\sqrt{3N}$ , respectively, where R is the maximum cell radios and  $R\sqrt{3N}$  is interference signal distance from the receiver. So, we can change the above equality with the following inequality:

$$C_{\text{avg}}^{[i]} \ge \int_{-\infty}^{+\infty} \frac{1}{4} \log \left( 1 + \frac{\delta^2 P_t / R^{\alpha}}{P_n + \delta_{\text{max}}^2 \left( \sum_j \frac{1}{(R\sqrt{3N})^{\alpha}} \right) P_t} \right) \times f_{\Delta}(\delta) d\delta, \tag{25}$$

where  $\neq i, j \in \mathcal{K}$ . If all interfering transmitters have the same distance to the receiver, and  $P_t \gg P_n$ , then the above inequality can be simplified as follows:

$$C_{\text{avg}}^{[i]} \geq \int_{-\infty}^{+\infty} \frac{1}{4} \log \left( 1 + \frac{\delta^2 P_t / R^{\alpha}}{P_n + \delta_{\text{max}}^2 \left( \frac{|\mathcal{K} - 1|}{(R\sqrt{3N})^{\alpha}} \right) P_t} \right) \times f_{\Delta}(\delta) d\delta,$$

$$\stackrel{(a)}{\approx} \int_{-\infty}^{+\infty} \frac{1}{4} \log \left( \frac{\delta^2 (3N)^{\frac{\alpha}{2}}}{\delta_{\text{max}}^2 (|\mathcal{K}| - 1)} \right) f_{\Delta}(\delta) d\delta$$

$$= \int_{-\infty}^{+\infty} \frac{1}{4} \log \left( \delta^2 \right) f_{\Delta}(\delta) d\delta + \frac{1}{4} \log \left( \frac{(3N)^{\frac{\alpha}{2}}}{\delta_{\text{max}}^2 (|\mathcal{K}| - 1)} \right),$$
(26)

where  $j \neq i, j \in \mathcal{K}$  and (a) comes from the assumption that  $P_t \gg P_n$ .

Remark 3: Here, we make the assumption that  $P_t\gg P_n$  in order to simplify the expression for the saturation point (the point beyond which we do not follow the pre-log factor of K/2), and obtain some insights as we discuss below. The motivation for this assumption is that at the saturation point, the interference power is the main bottleneck for communications.

From the above equations and (23) where  $\delta_{\max} < 2^{-\left(\frac{M}{|\mathcal{K}|-1}-1.5\right)\log 3}\sigma_H$ , we can conclude that:

$$C_{\text{avg}}^{[i]} \ge \int_{-\infty}^{+\infty} \frac{1}{4} \log \left(\delta^2\right) f_{\Delta}(\delta) d\delta + \left(\frac{M}{2(|\mathcal{K}|-1)} - \frac{1.5}{2}\right) \log 3 + \frac{\alpha}{8} \log 3N - \frac{1}{4} \log \left((|\mathcal{K}|-1)\sigma_H\right). \tag{27}$$

Assuming  $\sigma_H=1$ , the total average capacity of  $C_{\rm avg}$  can be lower bounded by  $|\mathcal{K}|C_{\rm avg}^{[k]}$  as follows:

$$C_{\text{avg}} \ge \int_{-\infty}^{+\infty} \frac{|\mathcal{K}|}{4} \log \left(\delta^{2}\right) f_{\Delta}(\delta) d\delta + \frac{M - 1.5(|\mathcal{K}| - 1)}{2} \log 3 + \frac{\alpha|\mathcal{K}|}{8} \log 3N - \frac{|\mathcal{K}|}{4} \log \left(|\mathcal{K}| - 1\right). \tag{28}$$

In the above lower-bound, we have four terms that can be interpreted as follows:

- $\int_{-\infty}^{+\infty} \frac{|\mathcal{K}|}{4} \log(\delta^2) f_{\delta}(\delta) d\delta$ : This term captures the multi-path gain of the environment at the antenna, see Fig. 5. We note that with beamforming, such gains would disappear;
- <sup>M</sup>/<sub>2</sub> log 3: This term indicates the rate that can be achieved from the number of antenna sub-elements. It is interesting that without having multi-channel processing (i.e. joint processing), we still obtain the benefit multi-channel processing from the new proposed antenna structure with only one RF chain. The term log 3/2 in this relation comes from having three different states for each sub-element across two times;
- $\frac{\alpha|\mathcal{K}|}{8} \log 3N$ : This term indicates the rate achieved through the path-loss exponent and the frequency reuse

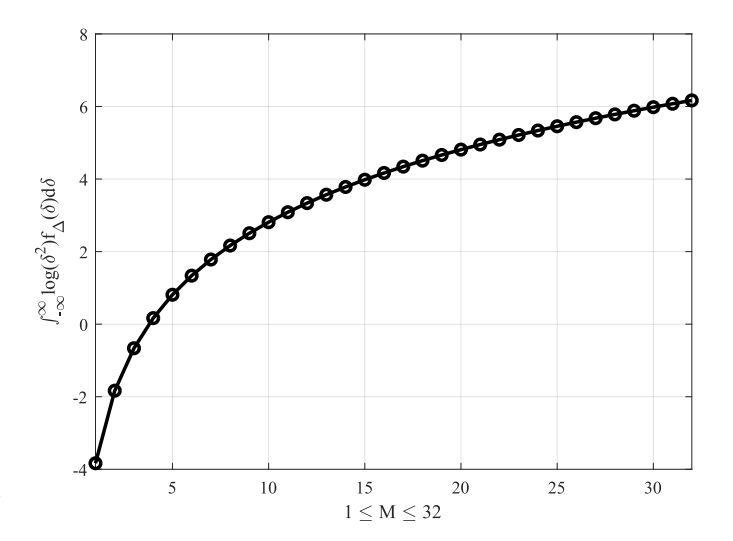


Fig. 5. Numerical solution for  $\int_{-\infty}^{+\infty} \log\left(\delta^2\right) f_{\Delta}(\delta) d\delta$  with different number of sub-elements  $1 \leq M \leq 32$ , where  $f_{\Delta}(\delta)$  has a Gaussian distribution with zero mean and variance of  $\frac{M}{2}$ .

factor, which can help the receivers reduce the effect of of interference signals;

•  $-\frac{|\mathcal{K}|}{4} \log(|\mathcal{K}| - 1) - \frac{1.5(|\mathcal{K}| - 1)}{2} \log 3$ : This term represents the negative impact of interfering signals in the transmission environment, which reduces the chance of finding proper channel conditions at the receivers.

#### C. Outage Capacity Analysis

In this subsection, we analyze the outage capacity of our technique for different values of  $P_t$ . We define  $(1 - \epsilon)$  outage capacity for each user as follows:

$$C_{1-\epsilon} = \{ R_t : P(R_t \ge C_h) \ge 1 - \epsilon \},$$
 (29)

where  $R_t$  is the transmission rate in which there exist a state among  $\frac{3^M-1}{2}$  different states with channel capacity of  $C_h$  with the probability greater than  $1-\epsilon$ . If we assume Gaussian distribution for  $f_{\Delta}(\delta)$  with variance of  $\frac{M}{2}\sigma_H^2$ , the outage capacity can be calculated as follows:

$$C_{1-\epsilon} = \frac{1}{4} \log \left( 1 + \frac{\Delta_{\epsilon}^2 P_t / R^{\alpha}}{P_n + \delta_{\max}^2 \left( \frac{|\mathcal{K} - 1|}{(R\sqrt{3N})^{\alpha}} P_t \right)} \right), \quad (30)$$

where  $\Delta_{\epsilon}$  is a positive-valued  $\Delta$  for which  $1-\int_{-\Delta_{\epsilon}}^{\Delta_{\epsilon}} f_{\Delta}(\delta) d\delta \geq 1-\epsilon$ . From the first lemma, if we consider Gaussian distribution with variance  $\frac{M}{2}\sigma_H^2$  for  $f_{\Delta}(\delta)$ , the value of  $\Delta_{\epsilon}$  for specific value of  $\epsilon$  can be calculated using the inverse of Q-function as follows:

$$\Delta_{\epsilon} = \sqrt{\frac{M}{2}} \sigma_H Q^{-1} \left( \frac{1 - \epsilon}{2} \right). \tag{31}$$

# V. SEARCH ALGORITHM

In the previous section, we proved that using our antenna structure it is possible to (almost surely) create conditions to align most of interference signal power to within a small value  $\delta_{\rm max}$ . In order to materialize this scheme, we need

to search among  $3^M$  different reception sates to find the best switching state at each receiver. For cellular wireless network applications, we typically engage with not more than 3 interference signals and choosing M=8 is sufficient for our results. Therefore, in this small practical case, our scheme can be implemented using a brute-force search algorithm to go through all  $\frac{3^8-1}{2}=3280$  switch combinations to minimize the effect of interference signals and maximize the desired signal power. However, when networks are dense and we have more users, the brute-force search becomes impractical.

Before we discuss our search algorithm, we define the optimization problem this algorithm needs to solve. From our system model and definitions, let  $\bar{\gamma}^{[i]} = \left(\gamma_1^{[i]}, \gamma_2^{[i]}, \dots, \gamma_M^{[i]}\right)$  be a vector where  $\gamma_j^{[i]} \in \{-1, 0, 1\}$ . At  $\mathrm{RX}_i$ , the goal is to:

$$\max_{\bar{\gamma}^{[i]}} |h_{1i}^{[i]} \gamma_1^{[i]} + h_{2i}^{[1]} \gamma_2^{[i]} + \dots h_{Mi}^{[i]} \gamma_M^{[i]}|^2, \tag{32}$$

while

$$|h_{1j}^{[i]}\gamma_1^{[i]} + h_{2j}^{[i]}\gamma_2^{[i]} + \dots + h_{Mj}^{[i]}\gamma_M^{[i]}|^2 \le \delta_j^2, \ j \ne i, j \in \mathcal{K},$$
(33)

where  $\delta_j$  is a small positive real number. Another representation of this problem is as follows:

$$\max_{\bar{\gamma}^{[i]}} \frac{|\bar{\gamma}^{[i]} \cdot \bar{\mathbf{H}}^{[ii]}|^2}{\sum_{j \in \mathcal{K}} |\bar{\gamma}^{[i]} \cdot \bar{\mathbf{H}}^{[ij]}|^2},\tag{34}$$

where in the above equation,  $\mathbf{U} \cdot \mathbf{H}^{[i]}$  is the inner product between two vectors  $\mathbf{U}$  and  $\mathbf{H}^{[i]}$ . We refer to

$$\frac{|\bar{\gamma}^{[i]} \cdot \bar{\mathbf{H}}^{[ii]}|^2}{\sum_{i \in \mathcal{K}} |\bar{\gamma}^{[i]} \cdot \bar{\mathbf{H}}^{[ij]}|^2}$$
(35)

as the *score function*. Next,  $\mathbf{H}^{[i]}$  can be expanded as follows:

$$\mathbf{H}^{[i]} = \left(h_1^{[i]}, h_2^{[i]}, \dots, h_M^{[i]}\right). \tag{36}$$

It is straightforward to see that a simple brute-force search algorithm has a complexity of  $\frac{3^M-1}{2},$  where the division by 2 comes from the fact that if  $\bar{\gamma}_*^{[i]}$  is the optimum vector (except all-zero vector which is not a solution) for our optimization problem, then  $-\bar{\gamma}_*^{[i]}$  is also an optimum vector. For large values of M, a brute-force search algorithm would be hard to implement.

# A. Proposed Search Algorithm

We propose a state search method in which all switching states of the  $i^{th}$  receiver generate a set  $\Gamma^{[i]}=\{\gamma_1^{[i]},\gamma_2^{[i]},\ldots,\gamma_M^{[i]}\}$  with  $\gamma_j^{[i]}\in\{-1,0,1\}$ . Our algorithm takes the following steps:

Step1: We generate  $\binom{M}{L}$  different sates<sup>4</sup> of  $\mathcal{F}_r^{[i]}, 1 \leq r \leq \binom{M}{L}$  where each state represents a set in which  $|\mathcal{F}_r^{[i]}| = L$  and  $\mathcal{F}_r^{[i]} \subset \Gamma^{[i]}$ . In other words, we select a subset of size L of sub-elements at each receive antenna out of M different sub-elements.

 $^4$ We assume M is divisible by L.

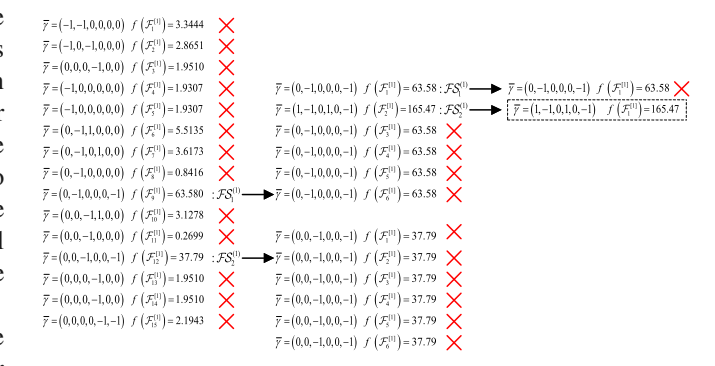


Fig. 6. The nodes with the arrows placed close to them indicate survived subsets and selected parents to generate offsprings. At each stage,  $N_s$  offsprings with the highest score function survive to continue the process. In this example, we used  $N_s = L = 2$ .

Step2: At the first stage, using a simple brute-force search algorithm, we calculate the score function for different subsets of  $\mathcal{F}_r^{(1)}$ ,  $1 \leq r \leq \binom{M}{L}$  and we select  $N_s$  survived states (parents) with highest score functions. We call them survived subsets of  $\{\mathcal{FS}_1^{(1)}, \mathcal{FS}_2^{(1)}, \ldots, \mathcal{FS}_{N_s}^{(1)}\}$  from the first stage. The complexity of this step is  $\frac{3^L-1}{2}\binom{M}{L}$ .

*Note:* When we calculate the *score function* for each state, we set all other elements in the set  $\Gamma^{[i]} \setminus \mathcal{F}_r$  to zero.

Step 3: For every survived subset, we generate new subsets of  $\mathcal{F}_r^{(2)}$ ,  $1 \leq r \leq \binom{M-L}{L}$  from the remaining members of  $\Gamma^{[i]} \setminus \mathcal{FS}_r^{(1)}$  which we refer to as the offspring of the parents from the previous stage. Similar to previous step, we choose  $N_s$  of them with highest score function as new parents and survived subsets.

Step 4: We repeat step 3 until no subsets are left.

Fig. 6 shows our proposed searching algorithm to find a (possibly locally optimal) vector  $\bar{\gamma}^{[i]}$  to maximize our *score* function.

# B. Complexity of the Proposed Search Algorithm

As we discussed earlier, a simple brute-force search algorithm needs to go through all  $\frac{3^M-1}{2}$  switch combinations to find the optimum solution. In this subsection, we analyze the complexity of our proposed search algorithm. At the first stage, we need to search among  $\binom{M}{L}$  subsets where for each subset using a simple brute-force algorithm, the algorithm searches among  $\frac{3^L-1}{2}$  switch combinations. Therefore, for the first step, we have a complexity of  $\frac{3^L-1}{2}\binom{M}{L}$ . At the second stage, we have  $N_s$  survived parents where for each parent we need to generate  $\binom{M-L}{L}$  subsets. Similar to the previous stage, we need to search among  $\frac{3^L-1}{2}$  searching point. Therefore, in this stage, we have a complexity of  $N_s\frac{3^L-1}{2}\binom{M-L}{L}$ . In general, during the  $i^{th}$  stage, we have the following complexity:

$$N_s \frac{3^L - 1}{2} \binom{M - (i - 1)L}{L}. \tag{37}$$

Finally, during the last stage, we have a complexity of  $\frac{3^L-1}{2}$  (there is no choice to select among the subsets). Therefore,

the total complexity of our algorithm can be calculated as follows:

$$\sum_{i=1}^{\frac{M}{L}-1} N_s \frac{3^L - 1}{2} \binom{M - (i-1)L}{L} + \frac{3^L - 1}{2}.$$
 (38)

If M is sufficiently greater than  $N_s$  and L, then the complexity order of the term in (38) can be upper bounded as follows:

$$\sum_{i=1}^{\frac{M}{L}-1} N_s \frac{3^L - 1}{2} \binom{M - (i-1)L}{L} + \frac{3^L - 1}{2} \\
\leq \sum_{i=1}^{\frac{M}{L}-1} N_s \frac{3^L - 1}{2} \frac{(M - (i-1)L)^L}{L^L} + \frac{3^L - 1}{2} \\
\approx \sum_{i=1}^{\frac{M}{L}-1} N_s \frac{3^L - 1}{2} \left(\frac{M}{L} - (i-1)\right)^L + \frac{3^L - 1}{2} \\
\leq \mathcal{O}\left(M^{L+1}\right). \tag{39}$$

As an example, for  $M=32,\,L=2,\,$  and  $N_s=5,\,$  the complexity of our proposed search algorithm at each receiver is 57104 which is  $1.6\times10^{10}$  times faster than the simple brute-force search algorithm.

As another example, consider a 3-user interference channel in which the channel vectors at the first receiver has the following form:

$$\begin{split} \bar{\mathbf{H}}^{[11]} = & [+1.409, +1.417, +0.671, -1.207, +0.717, +1.6302], \\ \bar{\mathbf{H}}^{[12]} = & [+0.488 + 1.034, +0.726, -0.303, +0.293, -0.7873], \\ \bar{\mathbf{H}}^{[13]} = & [+0.888, -1.147, -1.068, -0.809, -2.944, 1.4384]. \end{split}$$

$$(40)$$

The brute-force search algorithm would go through  $3^6=729$  switch combinations. Setting  $\bar{\gamma}^{[1]}=(-1,1,0,1,-1,0)$ , we can reach a *score function* of  $\frac{\Delta^2}{\delta^2}=293.5$ . Now, we want to test our proposed search algorithm by setting  $N_s=2$  and L=2. In this case, the first receiver generate  $\binom{6}{2}=15$  subsets as follows:

$$\begin{split} \mathcal{F}_{1}^{[1]} &= \{\gamma_{1}^{[1]}, \gamma_{2}^{[1]}\}, \ \mathcal{F}_{2}^{[1]} &= \{\gamma_{1}^{[1]}, \gamma_{3}^{[1]}\}, \ \mathcal{F}_{3}^{[1]} &= \{\gamma_{1}^{[1]}, \gamma_{4}^{[1]}\} \\ \mathcal{F}_{4}^{[1]} &= \{\gamma_{1}^{[1]}, \gamma_{5}^{[1]}\}, \ \mathcal{F}_{5}^{[1]} &= \{\gamma_{1}^{[1]}, \gamma_{6}^{[1]}\}, \ \mathcal{F}_{6}^{[1]} &= \{\gamma_{2}^{[1]}, \gamma_{3}^{[1]}\} \\ \mathcal{F}_{7}^{[1]} &= \{\gamma_{2}^{[1]}, \gamma_{4}^{[1]}\}, \ \mathcal{F}_{8}^{[1]} &= \{\gamma_{2}^{[1]}, \gamma_{5}^{[1]}\}, \ \mathcal{F}_{9}^{[1]} &= \{\gamma_{3}^{[1]}, \gamma_{4}^{[1]}\} \\ \mathcal{F}_{10}^{[1]} &= \{\gamma_{2}^{[1]}, \gamma_{6}^{[1]}\}, \ \mathcal{F}_{11}^{[1]} &= \{\gamma_{3}^{[1]}, \gamma_{5}^{[1]}\}, \ \mathcal{F}_{12}^{[1]} &= \{\gamma_{3}^{[1]}, \gamma_{6}^{[1]}\}, \\ \mathcal{F}_{13}^{[1]} &= \{\gamma_{4}^{[1]}, \gamma_{5}^{[1]}\}, \ \mathcal{F}_{14}^{[1]} &= \{\gamma_{4}^{[1]}, \gamma_{6}^{[1]}\}, \ \mathcal{F}_{15}^{[1]} &= \{\gamma_{5}^{[1]}, \gamma_{6}^{[1]}\}. \end{split}$$

For each subset above, using a simple brute-force search algorithm the receiver maximizes the *score function*  $f\left(\mathcal{F}_{j}^{[1]}\right), 1 \leq j \leq \binom{6}{2} = 15$ , and finds  $N_s = 2$  of them with highest *score function*. In the above example the maximum score function for each of the above subset can be calculated as what is achieved in the left column in Fig. 6. Given  $N_s = 2$ ,  $f\left(\mathcal{F}_{9}^{[1]}\right) = 63.580, \bar{\gamma}^{[1]} = (0, -1, 0, 0, 0, -1)$  and  $f\left(\mathcal{F}_{12}^{[1]}\right) = 37.7934, \bar{\gamma}^{[1]} = (0, 0, -1, 0, 0, -1)$  are the survived parents. From the first survived state

 $\mathcal{FS}_9^{[1]}=(0,-1,0,0,0,-1)$ , we have  $\binom{6-N_s}{2}=6$ ,  $N_s=2$  offspings as what have been calculated in the upper part of middle column in Fig. 6. From the survived state  $\mathcal{FS}_{12}^{[1]}=(0,0,-1,0,0,-1)$ , we have  $\binom{6-N_s}{2}=6$ ,  $N_s=2$  offsprings which have been calculated in the lower part of middle column in Fig. 6. From these relations, we can determine two further survived parents of  $f\left(\mathcal{F}_2^{[1]}\right)=165.4732$ ,  $\bar{\gamma}^{[1]}=(1,-1,0,1,0,-1)$  and  $f\left(\mathcal{F}_1^{[1]}\right)=63.58, \bar{\gamma}^{[1]}=(0,-1,0,0,0,-1)$  where each parent has one offspring. Finally, the *score function* is maximized by setting  $\bar{\gamma}_*^{[1]}=(1,-1,0,1,0,-1)$  and the value of *score function* is 165.4732 with a complexity of 256 compared to  $3^6=729$  for the bruteforce algorithm. The gap between our proposed algorithm and the brute-force algorithm grows as M increases. Nonetheless, our algorithm provides a "good" solution with much lower complexity in practical scenarios.

#### C. Random Search

We can also randomly choose different  $\bar{\gamma}^{[i]}$ 's at each receiver and select a vector that satisfies the minimum SINR condition at that receiver. For large values of M, we will show in the numerical results that the number of local maximums is sufficiently large to satisfy our conditions, which justifies the random search approach.

### VI. NUMERICAL AND SIMULATION RESULTS

In this section, we numerically analyze the performance of our proposed alignment strategy using the reconfigurable antenna of Section II-A. In our simulation results, we assume Rayleigh fading channels in which the real and the imaginary parts of the channel gains are modeled as independent and identically distributed zero-mean Gaussian processes. Since the real and the imaginary parts are independent of each other, our technique can be modified using simple 90-degree phase-shifters and RF switches. Therefore, we analyze only the real part of channel coefficients and the results can be generalized to complex channels. Basically, in all our simulations, we assume that there exist real-valued channel coefficients with Gaussian distribution among transmitters and receivers sub-elements.

Figure 7 shows a comparison between the Monte Carlo simulation with 1000 tries and our approximation in (42), where we have:

$$p\left(|\bar{\mathbf{H}}^{[ij]} \cdot \bar{\gamma}^{[j]}| < \delta\right) \approx \frac{2}{\sqrt{\pi M}} \frac{\delta_{\text{max}}}{\sigma_H}, \ j \text{ is a constant.}$$
(42)

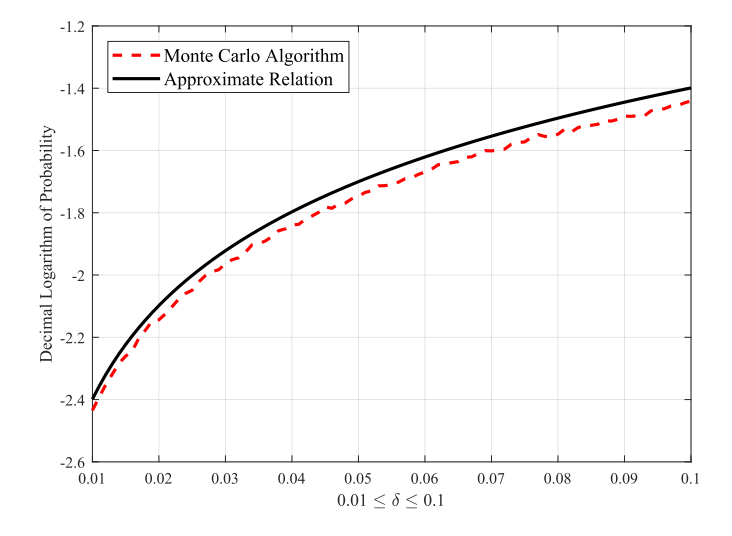
We observe that our approximation traces the simulation results within a small margin when  $0.01 \le \delta \le 0.1$ . As it is indicated in this figure, our approximation becomes more accurate for smaller values of  $\delta$ .

Figure 8 shows our average transmission rate for a 4-user interference channel with M=16 sub-elements at each receiver. In this figure, the red solid curve indicates the sum-rate of a 4-user interference channel with perfect CSI, the dashed blue curve indicate the sum rate of this channel

EXAMPLE OF 4-OSER IC AND THE HIGHEST SCORE JUICION VALUE					
K=4	M=8	M = 16	M = 24		
Brute-force algorithm	$\max \frac{\Delta^2}{\delta^2} = 100$	$\max \frac{\Delta^2}{\delta^2} = 16 \times 10^4$	$\max \frac{\Delta^2}{\delta^2} = 9 \times 10^6$		
Proposed strategy	$\max \frac{\mathring{\Delta}^2}{\mathring{\Delta}^2} = 100$	$\max \frac{\mathring{\Delta}^2}{\mathring{\Delta}^2} = 7.5 \times 10^4$	$\max \frac{\mathring{\Delta}^2}{\mathring{\Delta}^2} = 3 \times 10^6$		

TABLE II

EXAMPLE OF 4-USER IC AND THE HIGHEST Score function VALUE



Random search

Fig. 7. Comparison between our approximation of (42) and a Monte Carlo simulation with  $M=8,\,\sigma_H=1,$  and 1000 trials.

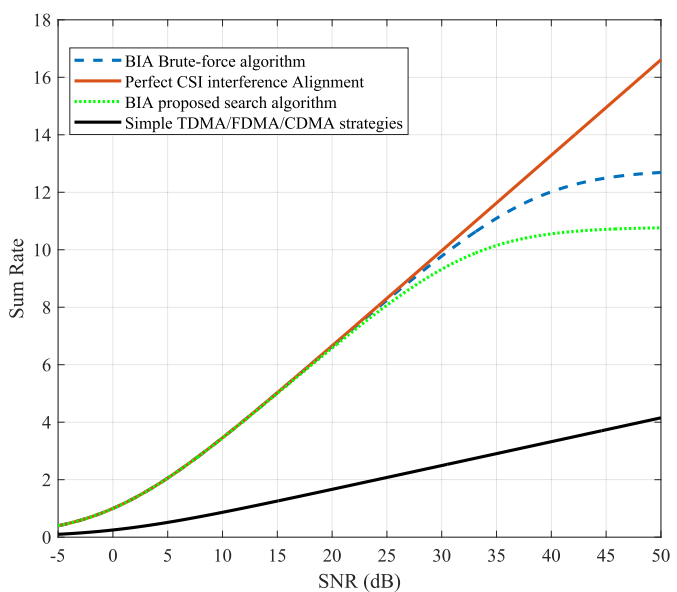
using our antenna structure and a simple brute-force algorithm. From (28), a lower-bound on the saturation rate can be calculated as follows:

$$C_{\text{avg}} \ge \int_{-\infty}^{+\infty} \frac{|\mathcal{K}|}{4} \log\left(\delta^2\right) f_{\Delta}(\delta) d\delta + \frac{M - 1.5(|\mathcal{K}| - 1)}{2} \log 3 + \frac{\alpha|\mathcal{K}|}{8} \log 3N - \frac{|\mathcal{K}|}{4} \log\left(|\mathcal{K}| - 1\right) = 11.66 \tag{43}$$

which matches what we observe in Figure 8. We should note that since in this case we do not use the interference reduction technique of cellular networks, the term  $\frac{\alpha |\mathcal{K}|}{8} \log 3N$  does not play a role in our relation (all the interference signals are received at the same power level).

We observe that our approach is able to trace the sum rate of the perfect interference alignment scheme for a practical SNR regime (i.e., SNR  $\leq 40 \mathrm{dB}$ ) without accessing channel state information at the transmitters. Since the simple brute-force search increases the complexity, we use our proposed algorithm, and as shown in Figure 8(a), for  $N_s=2$  and L=4, the number of trials is  $1.8\times10^4$  compared to the brute-force search with  $2.15\times10^7$  trials. This faster solution results in an acceptable 5dB performance degradation. We note that the perfect interference alignment scheme works for high SNR values and the bound is only included for comparison.

Figure 8(b) shows the outage capacity of our proposed strategy for different values of  $1-\epsilon$ . Not surprisingly, when  $\epsilon=0$ , we cannot find any value for  $R_t$  (transmission rate) in which the receiver can almost surely recover the transmitted data. Therefore, in this case, the value of  $C_{1-\epsilon}$  is zero. As  $\epsilon$  moves away from zero, the value of  $C_{1-\epsilon}$  starts to increase.



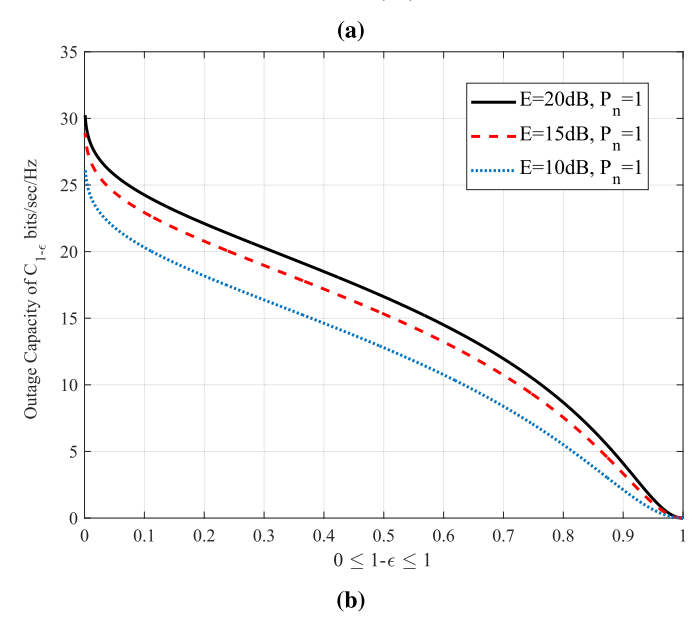


Fig. 8. (a) Comparison between our proposed strategy and interference alignment with perfect CSI in a 4-user IC; (b) The outage capacity as a function of  $(1-\epsilon)$  for M=12 and K=6 users and varying transmission power  $(\mathcal{E}=10,15,20\mathrm{dB})$ .

Table II and III show the performance and complexity of our proposed search algorithm compared to random search algorithm with a complexity of searching through  $\frac{3^8-1}{2}$  combinations and a simple brute-force algorithm with the complexity of  $\frac{3^M-1}{2}$ . For K=4 users, our approach provides a good solution, while reducing the complexity of search algorithm drastically. For M=16, our sum-rate has a saturation point

TABLE III  ${\it Complexity of Different Schemes Compared to Our Scheme With $L=4$ and $N_s=2$ }$ 

K=4	M=8	M = 16	M=24
Brute-force algorithm	$\frac{3^8-1}{2}$	$\frac{3^{16}-1}{2}$	$\frac{3^{24}-1}{2}$
Proposed strategy	5640	$1.9 \times 10^4$	$1.4 \times 10^{6}$
Random search	$\frac{3^8-1}{2}$	$\frac{3^8-1}{2}$	$\frac{3^8-1}{2}$

around 48dB and has a complexity of 19000, which with a basic 60-MHz processor can be calculated within 0.3ms. Considering channel coherence time of  $\frac{c}{fv}=6.25\mathrm{ms}$  for a receiver with a speed of  $v=30\mathrm{m/sec}$  and operation frequency of  $f=1.6\mathrm{GHz}$ , the search algorithm overhead would be a negligible part of signaling.

#### VII. CONCLUSION AND FUTURE WORK

In this paper, we proposed a distributed blind interference management strategy in K-user ICs that exploits the receiver-end diversity created by a switch-based reconfigurable antenna. A major difference between this antenna and other multiple-antenna structures is that it has only one RF chain, which prohibits joint processing. The proposed scheme allows transceivers to achieve higher average sum-rates without accessing CSI at the transmitters, and matches the promised high-SNR gains of Interference Alignment for finite SNR values. We designed our scheme such that interference signals align to within a small margin. We showed that when the number of sub-elements at the receivers increases, the chance of finding proper channel conditions to eliminate most of interfering signal power increases. We then analyzed the average achievable sum-rate of our approach, and we proposed an efficient algorithm to search among different reception states. We showed that by a small sacrifice in SINR, we can find proper states with lower complexity. Through numerical analysis, we showed that our new approach enables interference mitigating without the main drawbacks of prior results. One can extend the results of this paper to other network architectures or protocols to improve data reception rates. Another direction is to analyze the antenna structure with different types of antenna sub-elements or increase the number of reception switching state with phase-shifters or attenuators.

# APPENDIX A PROOF OF THE FIRST LEMMA

*Proof:* The vector  $\bar{\gamma}^{[i]} = \left(\gamma_1^{[i]}, \dots, \gamma_M^{[i]}\right)$  has  $3^M$  different shapes in which  $\gamma_k^{[i]} \in \{-1,0,1\}$ . The inner product of two vectors  $\bar{\mathbf{H}}^{[ij]}$  and  $\bar{\gamma}^{[i]}$  can be expanded as follows:

$$\bar{\mathbf{H}}^{[ij]} \cdot \bar{\gamma}^{[i]} = \sum_{m=1}^{M} h_m^{[ij]} \gamma_m^{[j]}.$$
 (44)

Therefore, we have:

$$\operatorname{var}\left(\bar{\mathbf{H}}^{[ij]} \cdot \bar{\gamma}^{[i]}\right) = \operatorname{var}\left(\sum_{m=1}^{M} h_{m}^{[ij]} \gamma_{m}^{[i]}\right)$$
$$= \sum_{m=1}^{M} \operatorname{var}\left(h_{m}^{[ij]}\right) |\gamma_{m}^{[i]}| = \sigma_{H}^{2} \sum_{m=1}^{M} |\gamma_{m}^{[i]}|$$
(45)

If we consider uniform distribution among different state of the vector  $\bar{\gamma}^{[i]}$ , the average variance of  $\operatorname{var}\left(\bar{\mathbf{H}}^{[ij]}\cdot\bar{\gamma}^{[i]}\right)$  can be calculated as follows:

$$\bar{\operatorname{var}}\left(\bar{\mathbf{H}}^{[ij]} \cdot \bar{\gamma}^{[i]}\right) = \mathbb{E}\left(\sigma_H^2 \sum_{m=1}^M |\gamma_m^{[i]}|\right) \tag{46}$$

$$= \sigma_H^2 \sum_{l=0}^{M} p\left(\sum_{m=1}^{M} |\gamma_m^{[i]}| = l\right) l, \quad (47)$$

where  $0 \leq l \leq M$ . If we consider uniform distribution among different switching states, the value of  $p\left(\sum_{m=1}^{M}|\gamma_{m}^{[i]}|=l\right)$  can be calculated from  $\frac{\binom{M}{M-l}}{2^M}$ . In which, the value of  $\binom{M}{M-l}$  counts the number of states in which the vector  $\bar{\gamma}^{[i]}$  contains M-l zeros and  $2^M$  indicates total number of states for  $|\bar{\gamma}^{[i]}|$  which contains zero or one. Therefore, we can conclude that:

$$\bar{\operatorname{var}}\left(\bar{\mathbf{H}}^{[ij]} \cdot \bar{\gamma}^{[i]}\right) = \frac{\sum_{l=0}^{M} \binom{M}{M-l} l}{2^{M}} \sigma_{H}^{2}, \tag{48}$$

if we substitute M-l with l', then

$$\operatorname{var}\left(\bar{\mathbf{H}}^{[ij]} \cdot \bar{\gamma}^{[i]}\right) = \frac{\sum_{l'=0}^{M} \binom{M}{l'} (M - l')}{2^{M}} \sigma_{H}^{2} = \frac{M}{2} \sigma_{H}^{2}$$
(49)

which completes the proof.

# $\begin{array}{c} \text{Appendix B} \\ \text{Proof of the Second Lemma} \end{array}$

*Proof:* As it discussed in the previous lemma for different vectors,  $\bar{\gamma}^{[i]}$ , the distribution of  $\bar{\mathbf{H}}^{[ij]} \cdot \bar{\gamma}^{[i]}$  can be approximated by Gaussian distribution with zero mean and variance V. So, we have:

$$p\left(|\bar{\mathbf{H}}^{[ij]} \cdot \bar{\gamma}^{[i]}| < \delta\right) = \int_{-\delta}^{\delta} \frac{1}{\sqrt{2\pi V}} e^{-\frac{r^2}{2V}} dr$$

$$\stackrel{(a)}{\approx} \int_{-\delta}^{\delta} \frac{1}{\sqrt{2\pi V}} \left(1 - \frac{r^2}{2V} + \mathcal{O}\left(\frac{r^4}{V^3}\right)\right) dr$$

$$= \frac{2}{\sqrt{2\pi}} \frac{\delta}{\sigma} - \frac{2}{3\sqrt{2\pi}} \frac{\delta^3}{\sigma^3} + \mathcal{O}\left(\frac{\delta^5}{\sigma^5}\right)$$
(50)

where the approximation (a) comes from the Taylor series expansion of the term  $e^{-\frac{r^2}{2V}}$  and in all the above equations  $\sigma$  is equal to  $\sqrt{V}$ .

#### REFERENCES

- J. M. C. Brito, "Trends in wireless communications towards 5G networks—The influence of e-health and IoT applications," in *Proc. Int. Multidisciplinary Conf. Comput. Energy Sci. (SpliTech)*, Jul. 2016, pp. 1–7.
- [2] Z. Xiao, X. G. Xia, and L. Bai, "Achieving antenna and multipath diversities in GLRT-based burst packet detection," *IEEE Trans. Signal Process.*, vol. 63, no. 7, pp. 1832–1845, Apr. 2015.

- [3] M. A. Maddah-Ali, A. S. Motahari, and A. K. Khandani, "Communication over MIMO X channels: Interference alignment, decomposition, and performance analysis," *IEEE Trans. Inf. Theory*, vol. 54, no. 8, pp. 3457–3470, Aug. 2008.
- [4] V. R. Cadambe and S. A. Jafar, "Interference alignment and degrees of freedom for the K-user interference channel," *IEEE Trans. Inf. Theory*, vol. 54, no. 8, pp. 3425–3441, Aug. 2008.
- [5] N. Zhao, F. R. Yu, M. Jin, Q. Yan, and V. C. M. Leung, "Interference alignment and its applications: A survey, research issues, and challenges," *IEEE Commun. Surveys Tuts.*, vol. 18, no. 3, pp. 1779–1803, 3rd Quart., 2016.
- [6] A. Falahati and M. Akbari, "Interference alignment in space, time and frequency: Achievable DoF analysis," *Electron. Lett.*, vol. 52, no. 3, pp. 204–206, Feb. 2016.
- [7] M. S. Afaqui, E. Garcia-Villegas, and E. Lopez-Aguilera, "IEEE 802.11ax: Challenges and requirements for future high efficiency WiFi," *IEEE Wireless Commun.*, vol. 24, no. 3, pp. 130–137, Jun. 2017.
  [8] S. A. Jafar, "Blind interference alignment," *IEEE J. Sel. Topics Signal*
- [8] S. A. Jafar, "Blind interference alignment," *IEEE J. Sel. Topics Signal Process.*, vol. 6, no. 3, pp. 216–227, Jun. 2012.
- [9] T. Gou, C. Wang, and S. A. Jafar, "Aiming perfectly in the dark-blind interference alignment through staggered antenna switching," *IEEE Trans. Signal Process.*, vol. 59, no. 6, pp. 2734–2744, Jun. 2011.
- [10] M. Johnny and M. R. Aref, "Sum degrees of freedom for the K-user interference channel using antenna switching," in *Proc. 21th Int. ITG* Workshop Smart Antennas (WSA), Mar. 2017, pp. 1–6.
- [11] M. Johnny and M. R. Aref, "BIA for the K-user interference channel using reconfigurable antenna at receivers," *IEEE Trans. Inf. Theory*, vol. 66, no. 4, pp. 2184–2197, Apr. 2020.
- [12] S. Begashaw, J. Chacko, N. Gulati, D. H. Nguyen, N. Kandasamy, and K. R. Dandekar, "Experimental evaluation of a reconfigurable antenna system for blind interference alignment," in *Proc. IEEE 17th Annu.* Wireless Microw. Technol. Conf. (WAMICON), Apr. 2016, pp. 1–6.
- [13] M. Johnny and M. R. Aref, "Blind interference alignment for the k-user siso interference channel using reconfigurable antennas," *IEEE Commun. Lett.*, vol. 22, no. 5, pp. 1046–1049, May 2018.
- [14] B. Nazer, M. Gastpar, S. A. Jafar, and S. Vishwanath, "Ergodic interference alignment," *IEEE Trans. Inf. Theory*, vol. 58, no. 10, pp. 6355–6371, Oct. 2012.
- [15] A. Leshem and U. Erez, "Ergodic spatial nulling for achieving interference free rates," in *Proc. IEEE Int. Symp. Inf. Theory (ISIT)*, Jul. 2019, pp. 1292–1296.
- [16] M. Johnny and A. Vahid, "Embedding information in radiation pattern fluctuations," in *Proc. IEEE Int. Symp. Inf. Theory (ISIT)*, Jun. 2020, pp. 1534–1539.
- [17] M. Johnny and A. Vahid, "Exploiting coherence time variations for opportunistic blind interference alignment," *IEEE Trans. Commun.*, vol. 68, no. 10, pp. 6054–6069, Oct. 2020.
- [18] A. Vahid and R. Calderbank, "Two-user erasure interference channels with local delayed CSIT," *IEEE Trans. Inf. Theory*, vol. 62, no. 9, pp. 4910–4923, Sep. 2016.
- [19] S.-C. Lin, I.-H. Wang, and A. Vahid, "No feedback, no problem: Capacity of erasure broadcast channels with single-user delayed CSI," in *Proc. IEEE Int. Symp. Inf. Theory (ISIT)*, Jul. 2019, pp. 1647–1651.
- [20] S.-C. Lin, I.-H. Wang, and A. Vahid, "Capacity of broadcast packet erasure channels with single-user delayed CSI," *IEEE Trans. Inf. Theory*, vol. 67, no. 10, pp. 6283–6295, Oct. 2021.
- [21] A. Vahid, I.-H. Wang, and S.-C. Lin, "Capacity results for erasure broadcast channels with intermittent feedback," in *Proc. IEEE Inf. Theory Workshop (ITW)*, Aug. 2019, pp. 1–5.
- [22] A. Vahid, S.-C. Lin, and I.-H. Wang, "Erasure broadcast channels with intermittent feedback," *IEEE Trans. Commun.*, early access, Aug. 5, 2021, doi: 10.1109/TCOMM.2021.3102648.
- [23] A. Vahid, I. Shomorony, and R. Calderbank, "Informational bottlenecks in two-unicast wireless networks with delayed CSIT," in *Proc. 53rd Annu. Allerton Conf. Commun., Control, Comput. (Allerton)*, Sep. 2015, pp. 1256–1263.
- [24] A. Vahid, "On the degrees-of-freedom of two-unicast wireless networks with delayed CSIT," *IEEE Trans. Inf. Theory*, vol. 65, no. 8, pp. 5176–5188, Aug. 2019.

- [25] H. Yang, W. Shin, and J. Lee, "Linear degrees of freedom of full-duplex cellular networks with reconfigurable antennas," *IEEE Trans. Wireless Commun.*, vol. 16, no. 11, pp. 7195–7206, Nov. 2017.
- [26] S. Kumar, J.-F. Chamberland, and G. H. Huff, "Reconfigurable antennas, preemptive switching and virtual channel management," *IEEE Trans. Commun.*, vol. 62, no. 4, pp. 1272–1282, Apr. 2014.
- [27] A. Grau, H. Jafarkhani, and F. D. Flaviis, "A reconfigurable multipleinput multiple-output communication system," *IEEE Trans. Wireless Commun.*, vol. 7, no. 5, pp. 1719–1733, May 2008.
- [28] R. Senanayake, P. J. Smith, P. A. Martin, and J. S. Evans, "Performance analysis of reconfigurable antenna arrays," *IEEE Trans. Commun.*, vol. 65, no. 6, pp. 2726–2739, Jun. 2017.
- [29] M. A. Maddah-Ali and D. Tse, "Completely stale transmitter channel state information is still very useful," *IEEE Trans. Inf. Theory*, vol. 58, no. 7, pp. 4418–4431, Jul. 2012.
- [30] A. Vahid, M. A. Maddah-Ali, and A. S. Avestimehr, "Approximate capacity of the two-user MISO broadcast channel with delayed CSIT," in *Proc. 51st Annu. Allerton Conf. Commun., Control, Comput. (Allerton)*, Oct. 2013, pp. 1136–1143.
- [31] A. Vahid, M. A. Maddah-Ali, and A. S. Avestimehr, "Approximate capacity region of the MISO broadcast channels with delayed CSIT," *IEEE Trans. Commun.*, vol. 64, no. 7, pp. 2913–2924, Jul. 2016.
- [32] T. S. Rappaport, Wireless Communications: Principles and Practice, vol. 2. Upper Saddle River, NJ, USA: Prentice-Hall, 1996.



Milad Johnny received the B.Sc. and M.Sc. degrees in electrical and communication engineering from Iran University of Science and Technology, Tehran, Iran, in 2010 and 2012, respectively, and the Ph.D. degree from Sharif University of Technology in 2018. Since 2012, he has been with the Information Systems and Security Laboratory (ISSL), Sharif University of Technology. From March 2016 to September 2016, he was a Visiting Student with the Coding Signal Transmission Laboratory (CSTL), Waterloo University, Waterloo, ON, Canada. His

research interests include coding and information theory, wireless communications, and signal and array processing. In 2019, he was awarded the highly prestigious 21st Khwarizmi Young Award, which is given annually by the Iranian Research Organization for Science and Technology (IROST) under the Ministry of Science, Research and Technology of Iran to individuals who have made outstanding achievements in research, innovation, and invention. Due to his outstanding research in the area of communication and wireless technology he was awarded by World Intellectual Property Organization (WIPO) in 2019.



Alireza Vahid (Senior Member, IEEE) received the B.Sc. degree in electrical engineering from Sharif University of Technology, Tehran, Iran, in 2009, and the M.Sc. and Ph.D. degrees in electrical and computer engineering from Cornell University, Ithaca, NY, USA, in 2012 and 2015 respectively. From 2015 to 2017, he worked as a Post-Doctoral Research Scientist at the Information Initiative at Duke University, Durham, NC, USA. He is currently an Assistant Professor of electrical engineering at the University of Colorado at Denver, Denver, CO, USA.

His research interests include network information theory, wireless communications, coding theory, and applications of coding theory in high-performance computer memory systems. He received the 2015 Outstanding Ph.D. Thesis Research Award, the 2010 Director's Ph.D. Teaching Award, Jacobs Scholar Fellowship in 2009 from Cornell University, Qualcomm Innovation Fellowship in 2013, and the Lab Venture Challenge Award in 2019.